

# Detection of Atrial Fibrillation Driver Locations Using CNN and Body Surface Potentials

Miguel Ángel Cámara-Vázquez<sup>a</sup>, Ismael Hernández-Romero<sup>a</sup>, Eduardo Morgado-Reyes<sup>a</sup>, María S Guillem<sup>b</sup>, Andreu M Climent<sup>b</sup>, Óscar Barquero-Pérez<sup>a</sup>

<sup>a</sup> Universidad Rey Juan Carlos, Fuenlabrada, Madrid, Spain

<sup>b</sup> ITACA Institute, Universitat Politècnica de València, València, Spain

## Abstract

*Atrial fibrillation (AF) is characterized by complex and irregular propagation patterns, and AF onset locations and drivers responsible for its perpetuation are main targets for ablation procedures. Several Deep Learning-based methods have proposed to detect AF, but the estimation of the atrial area where the drivers are found is a topic where further research is needed. In this work, we propose to estimate the zone where AF drivers are found from body surface potentials (BSPs) and Convolutional Neural Networks (CNN), modeling a supervised classification problem. Accuracy in the test set was 0.89 when using noisy BSPs (SNR=20dB), while the Cohen's Kappa was 0.85. Therefore, the proposed method could help to identify target regions for ablation using a non-invasive procedure, and avoiding the use of ECG Imaging (ECGI).*

## 1. Introduction

Atrial fibrillation (AF) is the most common type of arrhythmia found clinical practice. This condition affects more than 33 million patients in the world [1]. AF increases the risk of suffering embolism, cardiac failure, stroke or, in the worst of cases, death [2]. One of the clinical goals in AF patients is to restore sinus rhythm by ablation, where targets are AF onset locations and drivers responsible for AF perpetuation [3]. Several studies have proposed different strategies to locate AF drivers by applying ECG Imaging (ECGI) [4–6], but this approach still needs further improvement.

Machine Learning (ML) and Deep Learning (DL) techniques can be nowadays a useful tool when assessing different AF scenarios. Several studies have proposed different methodologies [7, 8] in terms of AF detection, but AF area detection were out of the scope. However, recent studies have proposed to detect AF drivers in the pulmonary veins (PVs) zones using decision trees and a 12-ECG lead set [9] or estimate the AF driver location using neural net-

works and 64 body surface potentials (BSPs) [10].

We propose to use Convolutional Neural Networks (CNNs), which accounts for spatial characteristics, to predict the area where the AF drivers are found using BSP signals. For this aim, we will address this problem as a supervised model from annotated realistic computerized AF models [10, 11].

The remaining of the paper is organized as follows. In Section 2 we introduce the computational models used for this study, the experimental set-up, performance metrics and Deep Learning architecture. Final results are summarized in Section 3 and in Section 4 main conclusions are presented.

## 2. Methods

### 2.1. Computerized Models

We used realistic computerized models of atria (N=2039 nodes) and torso (M=659 nodes) [6, 11, 12]. The geometrical model considered consists on a simplified single endocardium-epicardium layer for the atrial tissue. Atria and torso models were used to simulate 13 different AF propagation patterns in both left atria (LA) and right atria (RA), with different degree of simulated fibrosis (up to the 50% of the tissue), and driver positions: Posterior Left Atrial Wall (PLAW), Left Inferior Pulmonary Vein (LIPV), Left Superior Pulmonary Vein (LSPV), Right Inferior Pulmonary Vein (RIPV), Right Superior Pulmonary Vein (RSPV), Right Atrial Appendage (RAA) and Right Atria Free Wall (RAFW). Sampling rate of the signals was  $f_s = 500\text{Hz}$ , while their duration ranged from 2 to 5 seconds.

### 2.2. AF driver location as a classification problem

We divided the atria into 7 different regions [10, 13], and manually labeled the localization of the AF driver within the 7 regions for each time instant. If there is no driver

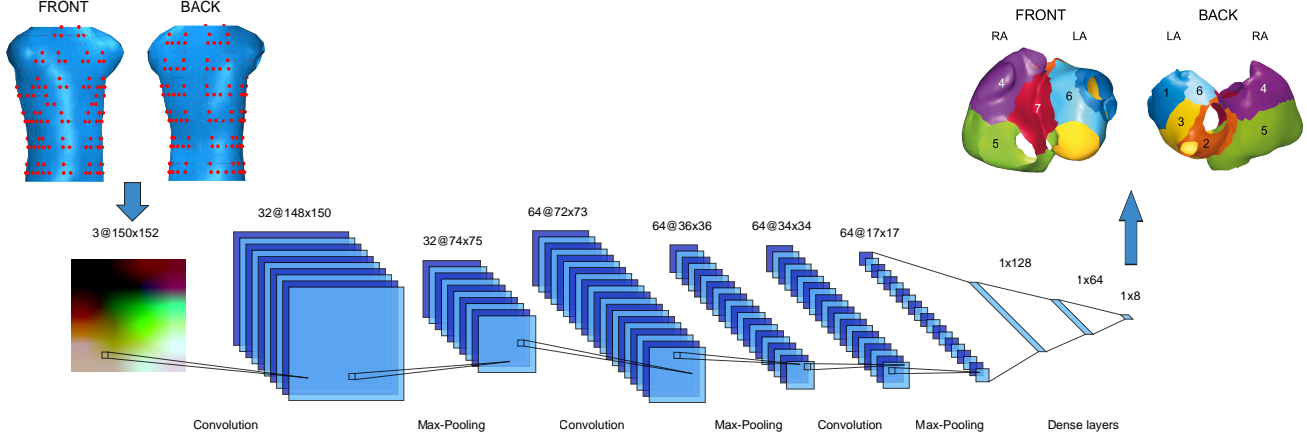


Figure 1. Schematic overview of the CNN-based proposed architecture.

found, the assigned label will be 0. Therefore, we transformed the AF driver location into a multi-classification supervised problem with 8 different classes.

Simulated BSPs were obtained by computing the forward problem of electrocardiography for each AF computerized model [6]. The electrical signals were referenced to the Wilson Central Terminal (WCT). To obtain noisy signals, we corrupted clean BSPs with additive Gaussian noise (different SNR) and filtered them using a 4<sup>th</sup>-order bandpass Butterworth filter ( $fc_1=3$  Hz and  $fc_2=30$ Hz) [6, 11]. Finally, a set of 64 electrodes from the whole torso geometry were selected to represent realistic multi-electrode vest used in electrophysiological studies (Figure 1).

To obtain final input data, we built a tensor that represents the layout of electrodes represented in Figure 1. For this purpose, we created tridimensional matrices of shape  $(6 \times 4 \times 3)$  from the BSP signals, one for each time instant. The first and last channel contain BSPs of the torso and back, respectively (24 electrodes each), and the second channel contains BSPs from the sides (16 electrodes distributed on the last 4 rows, while the rest are filled with zeroes). Finally, we performed a bilinear interpolation to create tensors with shape  $(150 \times 152 \times 3)$ .

### 2.3. Convolutional Neural Network (CNN) architecture

CNNs are a type of DL algorithm used mainly in image recognition and image classification. CNNs are able to exploit spatial correlations to extract relevant features, increasing classification performance [14].

The proposed CNN-based architecture is shown in Figure 1. Input data are tensors of shape  $(150 \times 152 \times 3)$ . We used three convolutional layers with 32, 64 and 64 filters with  $(3 \times 3)$  size. ReLU activation function was

used. Max-pooling is applied after each convolutional layer  $((2,2)$  window size). Finally, we added two dense layers of size (128, 64) units (ReLU activation function), while the output layer is a Softmax layer composed by 8 units to perform the classification.

### 2.4. Performance metrics

We used two metrics to assess the performance of the CNN model. The first one is the accuracy ( $Acc$ ), which is the fraction of well-classified drivers (true positives, TP) over the total of drivers (Total):

$$Acc = \frac{TP}{Total}$$

The second metric used is the Cohen's Kappa ( $\kappa$ ), which is a robust statistic used for measure the degree of agreement between two classifiers (in this case, the ground truth and CNN model) [15]. It is computed as:

$$\kappa = \frac{p_o - p_e}{1 - p_e}$$

where  $p_o$  is the relative agreement among raters, and  $p_e$  the hypothetical probability of chance agreement. A Cohen's Kappa score of 0 means the agreement that can be expected from random chance, while a score of 1 reflects perfect agreement between the raters. Finally, scores less than 0 means that there is less agreement than chance.

### 2.5. Experimental set-up

We addressed the classification problem considering each time instant as an independent sample. Therefore, the data set is composed of input data tensors of shape  $(150 \times 152 \times 3)$ , obtained from 64 BSP electrodes,  $\mathbf{x}_i$ , and their corresponding label  $y_i$  which can have values  $0, 1, \dots, 7$ .

To train the model, we split the data set in training (80%) and test (20%) sets, using hold-out validation during the training process (20%). Several atria regions are over-represented in the data set (imbalanced data). To address this issue, we weighted the classes accordingly to the probability of occurrence.

### 3. Results

We trained a CNN model using BSPs with SNR=20dB. The aim of this experiment is to simulate a realistic scenario.

In this case, we were able to locate the 98% and 89% of drivers in the training and test sets, respectively. In the same scenario, Cohen’s Kappa metric was 0.97 and 0.85. Figure 2 shows the confusion matrix obtained in this scenario. There, the problem with imbalanced data is showed, since the accuracy obtained on septum area (label 7) is 0.53.

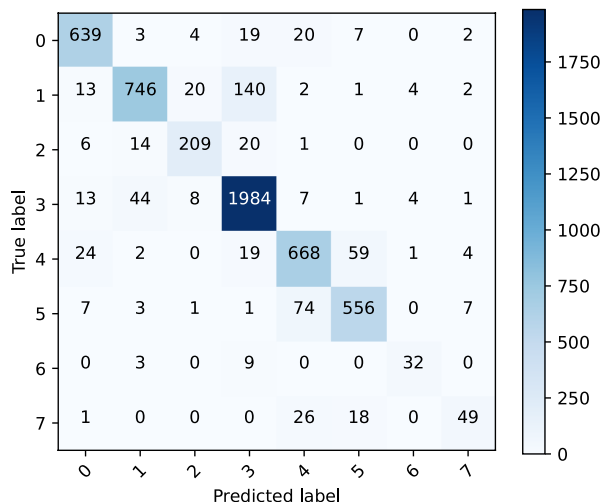


Figure 2. Confusion matrix obtained for the test set (SNR=20dB).

Test signals with different SNR were used to evaluate the noise robustness of the model. Scores are showed in Figure 3. Performance degraded severely when the SNR drops below 10dB, with an accuracy of 0.74 and a Cohen’s Kappa of 0.66. However, performance increases from SNR values higher than 10dB, obtaining scores over 0.84 (accuracy) and 0.8 (Cohen’s Kappa).

Finally, Figure 4 shows the probability of finding a driver in the different atrial regions for an example of AF model, considering time instants that belong to the test set. In this case, the model is able to correctly classify the area where the driver is found. Moreover, the area with the highest probability has 4.3 times more chances of containing a driver (0.57) than the one with the second highest probability found (0.13).

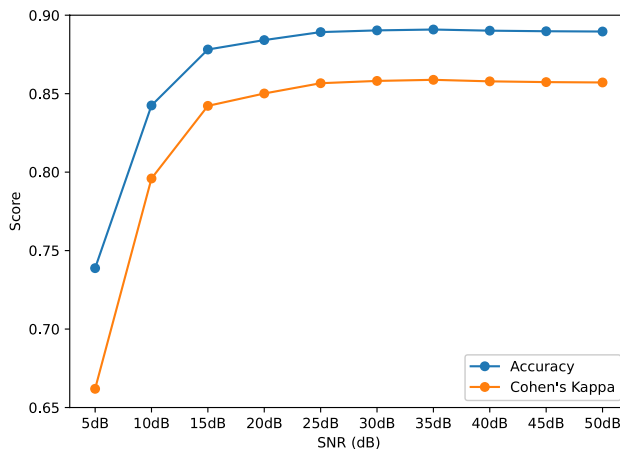


Figure 3. Performance metrics obtained with signals with different SNR (CNN trained with SNR=20dB).

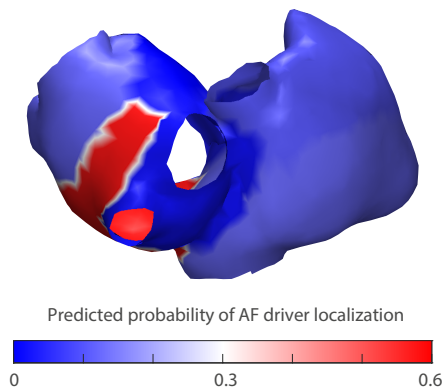


Figure 4. CNN model predicted probability for an example of AF model.

### 4. Discussion and conclusions

The proposed CNN-based method could help to identify the area where AF drivers are found using BSPs and avoiding the use of ECGL. This novel method has been demonstrated to be robust to noise, since its performance does not degrades significantly when using noisy BSPs.

However, this methodology has some drawbacks to be addressed. Our data set is composed by only 13 AF computerized models that represent different propagation patterns, but the distribution of drivers across the 7 defined atrial regions is not balanced. Therefore, the results on those less represented regions are going to be worse. This proposed division into 7 regions was used because it represents a clinical-based classification of the areas where the AF drivers are more commonly found and has been already clinically used to guide AF ablation strategies [13]. Nonetheless, our methodology can be easily extrapolated to other atrial geometry divisions based on a higher number of smaller regions, being able to get a higher resolution

in the driver classification.

Another important problem the ideal scenario we considered. Here, we trained the models with samples that belongs to the 13 AF models available. In a real situation, the CNN model will have to compute a prediction with a set of signals that was not used in the training process. Therefore, other types of training scenarios have to be tested (for example, splitting the data set by independent models instead of assuming time independence).

Regarding future research topics, the most important one is to apply this methodology with real patient data, where driver tagging can be difficult. In this scenario, Data Augmentation could be an useful tool to improve the generalization capability of the model. Finally, other DL architectures could be tested, like Recurrent Neural Networks (RNN), which are able to extract temporal characteristics of BSPs that are omitted when using CNNs.

## Acknowledgements

This work has been partially supported by: Ministerio de Ciencia e Innovación (PID2019-105032GB-I00), Instituto de Salud Carlos III, and Ministerio de Ciencia, Innovación y Universidades (supported by FEDER Fondo Europeo de Desarrollo Regional PI17/01106 and RYC2018-024346B-750), Consejería de Ciencia, Universidades e Innovación of the Comunidad de Madrid through the program RIS3 (S-2020/L2-622), EIT Health (Activity code 19600, EIT Health is supported by EIT, a body of the European Union) and the European Union's Horizon 2020 research and innovation program under the Marie Skłodowska-Curie grant agreement No. 860974.

## References

- [1] Chugh SS, Havmoeller R, Narayanan K, Singh D, Rienstra M, Benjamin EJ, Gillum RF, Kim YH, McAnulty JH, Zheng ZJ, Forouzanfar MH, Naghavi M, Mensah GA, Ezzati M, Murray CJ. Worldwide epidemiology of atrial fibrillation: A global burden of disease 2010 study. *Circulation* 2014;129(8):837–847. ISSN 00097322.
- [2] Fuster V, Rydén LE, Cannom DS, Crijns HJ, Curtis AB, Ellenbogen KA, Halperin JL. *Acc/aha/esc 2006 guidelines for the management of patients with atrial fibrillation: full text*. *Europace* 2006;8(9):651–745.
- [3] Guillem M, Climent A, Rodrigo M, Fernández-Avilés F, Atienza F, Berenfeld O. Presence and stability of rotors in atrial fibrillation: evidence and therapeutic implications. *Cardiovascular Res* 2016;109(4):480–492.
- [4] Haissaguerre M, Hocini M, Shah AJ, Derval N, Sacher F, Jais P, Dubois R. Noninvasive panoramic mapping of human atrial fibrillation mechanisms: A feasibility report. *Journal of Cardiovascular Electrophysiology* 2013; 24(6):711–717.
- [5] Rodrigo M, Climent AM, Liberos A, Calvo D, Fernández-Avilés F, Berenfeld O, et al. Identification of dominant excitation patterns and sources of atrial fibrillation by causality analysis. *Annals of Biomedical Engineering* 2016; 44(8):2364–2376.
- [6] Pedrón-Torrecilla J, Rodrigo M, Climent A, Liberos A, Pérez-David E, Bermejo J, et al. Noninvasive estimation of epicardial dominant high-frequency regions during atrial fibrillation. *J Cardiovascular Electrophysiol* 2016; 27(4):435–442.
- [7] Xiong Z, Stiles M, Zhao J. Robust ECG Signal Classification for the Detection of Atrial Fibrillation Using Novel Neural Networks. September 2017; .
- [8] Xia Y, Wulan N, Wang K, Zhang H. Detecting atrial fibrillation by deep convolutional neural networks. *Computers in Biology and Medicine* February 2018;93:84–92. ISSN 00104825.
- [9] Luongo G, Azzolin L, Schuler S, Rivolta MW, Almeida TP, Martínez JP, Soriano DC, Luik A, Müller-Edenborn B, Jaidi A, et al. Machine learning enables non-invasive prediction of atrial fibrillation driver location and acute pulmonary vein ablation success using the 12-lead eeg. *Cardiovascular Digital Health Journal* 2021;.
- [10] Cámara-Vázquez MÁ, Oter-Astillero A, Hernández-Romero I, Rodrigo M, Morgado-Reyes E, Guillem MS, Climent AM, Barquero-Pérez Ó. Atrial fibrillation driver localization from body surface potentials using deep learning. In 2020 Computing in Cardiology. IEEE, 2020; 1–4.
- [11] Figuera C, Suárez-Gutiérrez V, Hernández-Romero I, Rodrigo M, Liberos A, Atienza F, Guillem MS, Barquero-Pérez Ó, Climent AM, Alonso-Atienza F. Regularization Techniques for ECG Imaging during Atrial Fibrillation: A Computational Study. *Frontiers in Physiology* oct 2016; 7:466. ISSN 1664-042X.
- [12] García-Molla V, Liberos A, Vidal A, Guillem M, Millet J, González A, et al. Adaptive step {ODE} algorithms for the 3d simulation of electric heart activity with graphics processing units. *Computers in Biology and Medicine* 2014; 44:15 – 26.
- [13] Haissaguerre M, Hocini M, Denis A, Shah AJ, Komatsu Y, Yamashita S, et al. Driver domains in persistent atrial fibrillation. *Circulation* 2014;130(7):530–538.
- [14] Krizhevsky A, Sutskever I, Hinton GE. Imagenet classification with deep convolutional neural networks. *Communications of the ACM* 2017;60(6):84–90.
- [15] McHugh ML. Interrater reliability: the kappa statistic. *Biochemia Medica* October 2012;22(3):276–282. ISSN 1330-0962.

Address for correspondence:

Óscar Barquero-Pérez (oscar.barquero@urjc.es). Dept. III-D207, Camino del Molino, 5. 28943 - Fuenlabrada (Madrid), Spain.